Subaperture optical system testing

James E. Negro

Full aperture optical system wave-front accuracy obtainable from single or multiple subaperture wave-front measurements is analytically determined and illustrated with numerical examples. Insight gained from the analytic derivation and confirmed by the examples shows the effect of subaperture size, placement, and accuracy. The analysis also demonstrates that accurate full aperture aberrations (except tilt) can be estimated even with large uncertainty in relative subaperture tilt.

I. Introduction

An innovative large aperture optical test concept has been developed by Thunen and Kwon[1] which affords a lower cost alternative to traditional test approaches that use optical test flats or autocollimators having apertures at least as large as the optical system under test. For large aperture systems such as those now being conceptually designed for NASA and DOD, the optical test fixtures can be prohibitively expensive. Strong incentives exist for cheaper yet accurate large optical test alternatives.

The essence of the Thunen-Kwon[1] concept is the synthesis of a large test flat with an array of smaller test flats. Each small test flat has a good optical figure, but the overall figure of the test array may be quite poor due to inaccurate tilt alignment of the individual array flats. Thunen and Kwon have shown that the nontilt subaperture wave-front measurements are adequate to obtain good characterization of overall full aperture wave-front error, except for tilt. Their analysis is based on a digital computer numerical calculation of large aperture to small aperture wave-front aberration transformations. While this computer approach is essential for handling the large number of modes needed, it does not provide direct insight into the nature of the full aperture estimation problem and the key factors which affect the estimation process. In addition, no check or validation of the computer results is provided. In this section, an algebraic modeling approach is used to provide direct insights and an independent check of the simulation results.

The author is with Charles Stark Draper Laboratory, Inc., Systems & Optics Division, Advanced Systems Department, 555 Technology Square, Cambridge, Massachusetts 02139.

Received 6 January 1984.
0003-6935/84/121921-10$02.00/0.
© 1984 Optical Society of America.

Algebraic derivation of the sensitivity matrix is presented in Sec. II, and the full aperture Zernike mode estimation problem is formulated and solved in Sec. III. Both multiple subaperture and single central subaperture cases are considered.

II. Sensitivity Matrix Calculation

The essential element in multiple flat array subaperture testing is a sensitivity matrix S which represents the algebraic relationship between the full aperture aberration coefficients and subaperture aberration coefficients. Any convenient set of basis functions may be used to characterize aberrations, although an orthonormal basis set offers several advantages. We have used Zernike polynomials in this analysis: $\mathbf{SA} = \mathbf{a}$, where

$\mathbf{A} = (A_1, A_2, A_3, \ldots A_N)^T$, full aperture Zernike coefficients,

$\mathbf{a} = (a_1, a_2, a_3, \ldots a_m)^T$, subaperture Zernike coefficients,

and S is an $M \times N$ matrix having elements S_{mn}. We are interested in cases for which the subaperture may be arbitrarily placed within the full aperture. Its position within the full aperture is specified by its radial offset h from the full aperture center and the offset orientation angle α as shown in Fig. 1. Thus the sensitivity matrix elements are functions of h and α as well as the subaperture size r. In this section, the sensitivity matrix S relating the full aperture Zernike coefficients A_n to the coefficients a_n of a single subaperture is algebraically derived. Only ten modes are used to keep the algebraic analysis tractable.

The normalized circular Zernike mode definitions in Table I are used. We have ordered the mode sequences by their radial order, an aspect we shall find important in the sequel.

Algebraic derivation of the sensitivity matrix is based on the geometric relationships between the variables (ρ', θ') for the subaperture and the variables (ρ, θ) for the

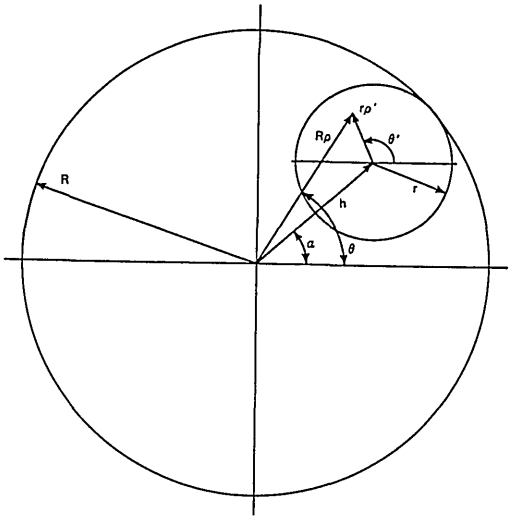

Fig. 1. Geometric relationship of a subaperture within the full aperture and definition of variables.

full aperture. From Fig. 1 the following geometric relationships apply:

$$R\rho\cos\theta = h\cos\alpha + r\rho'\cos\theta' \tag{1}$$

$$R\rho\sin\theta = h\sin\alpha + r\rho'\sin\theta', \tag{2}$$

where R is the radius of the full aperture, and r is the radius of the subaperture. These fundamental relationships are used to express each full aperture mode in terms of subaperture modes. Several examples illustrate the technique.

A. Full Aperture Tilt

The full aperture tilt is given by

$$Z_1 = 2\rho\cos\theta$$
$$= \frac{2}{R}\cdot R\rho\cos\theta = \frac{2}{R}(h\cos\alpha + r\rho'\cos\theta'),$$

where the last step follows using Eq. (1). Algebraically simplifying we obtain

$$Z_1 = 2\frac{h}{R}\cos\alpha + \left(\frac{r}{R}\right)2\rho'\cos\theta'. \tag{3}$$

The first term represents a phase piston term which depends on the fractional radial displacement (h/R) and displacement orientation angle α. As phase piston terms are unimportant in many optical systems, we shall ignore these components. The second term represents subaperture tilt. The tilt component is scaled by the ratio of subaperture to full aperture radii, i.e., (r/R). Thus one wave of full aperture tilt corresponds to only r/R waves of subaperture tilt.

Similarly,

$$Z_2 = 2\rho\sin\theta$$
$$= 2\frac{h}{R}\sin\alpha + \left(\frac{r}{R}\right)2\rho'\sin\theta'. \tag{4}$$

B. Full Aperture Focus

Full aperture terms having only a radial dependence can be derived from expressions for $(R\rho)^2$ obtained from Eqs. (1) and (2). Squaring these expressions and adding gives

$$(R\rho)^2 = (R\rho)^2(\cos^2\theta + \sin^2\theta)$$
$$= h^2 + r^2\rho'^2 + 2hr\rho'\cos(\theta' - \alpha).$$

Dividing both sides by R^2 and using trigonometric identities for the $\cos(\theta' - \alpha)$ term gives

$$\rho^2 = \left(\frac{h}{R}\right)^2 + \left(\frac{r}{R}\right)^2\rho'^2$$
$$+ \left(\frac{h}{R}\right)\left(\frac{r}{R}\right)(\cos\alpha 2\rho'\cos\theta' + \sin\alpha 2\rho'\sin\theta'). \tag{5}$$

This expression for ρ^2 is used to write the full aperture focus mode in terms of the subaperture modes:

$$Z_3 = \sqrt{3}(2\rho^2 - 1)$$
$$= \sqrt{3}\left[2\left(\frac{h}{R}\right)^2 - 1 + \left(\frac{r}{R}\right)^2\right] + \left(\frac{r}{R}\right)^2\sqrt{3}\,(2\rho'^2 - 1)$$
$$+ 2\sqrt{3}\left(\frac{h}{R}\right)\left(\frac{r}{R}\right)(\cos\alpha\, 2\rho'\cos\theta' + \sin\alpha\, 2\rho'\sin\theta'). \tag{6}$$

Equation (6) shows that the full aperture focus mode generates piston, tilt, and focus subaperture modes. Using primes to denote subaperture modes, we may write

$$Z_3 = \sqrt{3}\left[2\left(\frac{h}{R}\right)^2 - 1 + \left(\frac{r}{R}\right)^2\right] + \left(\frac{r}{R}\right)^2 Z_3'$$
$$+ 2\sqrt{3}\left(\frac{h}{R}\right)\left(\frac{r}{R}\right)[\cos\alpha Z_1' + \sin\alpha Z_2']. \tag{7}$$

Equation (7) shows that subaperture focus component scales as $(r/R)^2$ times the full aperture component and

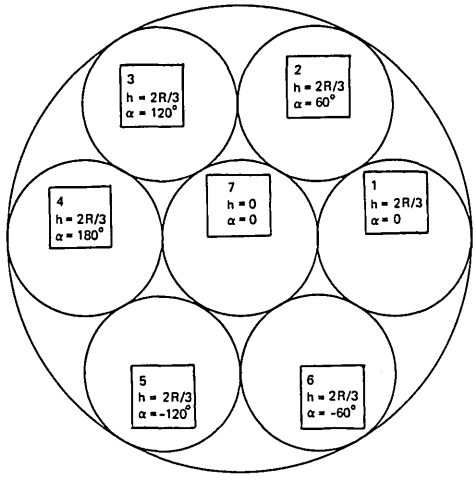

Fig. 2. Placement of seven subapertures within the full aperture for the multiple subaperture optical test concept.

Table II. Subaperture Zernike Mode Sensitivity Coefficients for Full Aperture Zernike Mode Aberrations

$S(\alpha,h) =$

$\frac{r}{R}$	0	$2\sqrt{3}\,\frac{h}{R}\frac{r}{R}\cos\alpha$	$\sqrt{6}\,\frac{h}{R}\frac{r}{R}\sin\alpha$	$3\sqrt{2}\,(\frac{r}{R})\cdot\left[(\frac{h}{R})^2(1+2\cos^2\alpha)+\frac{2}{3}(\frac{r}{R})^2-\frac{2}{3}\right]$	$3\sqrt{2}\,(\frac{h}{R})\frac{2r}{R}\sin 2\alpha$	$3\sqrt{2}\,(\frac{h}{R})\frac{2r}{R}\cos 2\alpha$	$12\sqrt{5}\,(\frac{h}{R})(\frac{r}{R})\cdot\left[(\frac{h}{R})^2+\frac{2}{3}(\frac{r}{R})^2-\frac{1}{2}\right]\cos\alpha$
0	$\frac{r}{R}$	$2\sqrt{3}\,\frac{h}{R}\frac{r}{R}\sin\alpha$	$\sqrt{6}\,\frac{h}{R}\frac{r}{R}\cos\alpha$	$3\sqrt{2}(\frac{h}{R})\frac{2r}{R}\sin 2\alpha$	$3\sqrt{2}\,(\frac{r}{R})\cdot\left[(\frac{h}{R})^2(1+2\sin^2\alpha)+\frac{2}{3}(\frac{r}{R})^2-\frac{2}{3}\right]$	$-3\sqrt{2}\,(\frac{h}{R})\frac{2r}{R}\sin 2\alpha$	$12\sqrt{5}\,(\frac{h}{R})(\frac{r}{R})\cdot\left[(\frac{h}{R})^2+\frac{2}{3}(\frac{r}{R})^2-\frac{1}{2}\right]\sin\alpha$
0 0		$(\frac{r}{R})^2$	0	$2\sqrt{6}\,\frac{h}{R}(\frac{r}{R})^2\cos\alpha$	$2\sqrt{6}\,\frac{h}{R}(\frac{r}{R})^2\sin\alpha$	0	$\left[4(\frac{h}{R})^2+(\frac{r}{R})^2-1\right]\cdot\sqrt{15}\,(\frac{r}{R})^2$
0 0		0	$(\frac{r}{R})^2$	$2\sqrt{3}\,\frac{h}{R}(\frac{r}{R})^2\cos\alpha$	$-2\sqrt{3}\,\frac{h}{R}(\frac{r}{R})^2\sin\alpha$	$2\sqrt{3}\,\frac{h}{R}(\frac{r}{R})^2\cdot\cos 2\alpha$	$2\sqrt{30}\,(\frac{h}{R})^2(\frac{r}{R})^2\cdot\cos 2\alpha$
0 0		0	0	$2\sqrt{3}\,\frac{h}{R}(\frac{r}{R})^2\sin\alpha$	$2\sqrt{3}\,\frac{h}{R}(\frac{r}{R})^2\cos\alpha$	$2\sqrt{3}\,\frac{h}{R}(\frac{r}{R})^2\cdot\sin 2\alpha$	$2\sqrt{30}\,(\frac{h}{R})^2(\frac{r}{R})^2\cdot\sin 2\alpha$
0 0		0	0	$(\frac{r}{R})^3$	0	0	$2\sqrt{10}\,(\frac{h}{R})(\frac{r}{R})^3\cdot\cos\alpha$
0 0		0	0	0	$(\frac{r}{R})^3$	0	$2\sqrt{10}\,(\frac{h}{R})(\frac{r}{R})^3\cdot\sin\alpha$
0 0		0	0	0	0	$(\frac{r}{R})^3$	0
0 0		0	0	0	0	0	0
0 0		0	0	0	0	0	$(\frac{r}{R})^4$
		A_3	A_4	A_5	A_6	A_7	A_8 A_9 A_{10}

Full Aperture Mode

Table I. Zernike Mode Definitions Used for Sensitivity Matrix Calculations (Unit Disk Normalization)

$z_1 = 2\rho\cos\theta$

$z_2 = 2\rho\sin\theta$

$z_3 = \sqrt{3}\,[2\rho^2 - 1]$ — Subaperture

$z_4 = \sqrt{6}\,\rho^2\cos 2\theta$ — $\rho \to \rho' = x/r$

$z_5 = \sqrt{6}\,\rho^2\sin 2\theta$ — $\theta \to \theta'$

$z_6 = \sqrt{8}\,[3\rho^2 - 2]\rho\cos\theta$ — Full Aperture

$z_7 = \sqrt{6}\,[3\rho^2 - 2]\rho\cos\theta$ — $\rho \to x/R$

$z_8 = \sqrt{8}\,\rho^3\cos 3\theta$ — $\theta \to \theta$

$z_9 = \sqrt{8}\,\rho^3\sin 3\theta$

$z_{10} = \sqrt{5}\,[6\rho^4 - 6\rho^2 + 1]$

Table III. Subaperture Placement Parameters for the Multiple Subaperture Flat Optical Test Configuration

Subaperture Number k	Subaperture Offset h_k	Offset Orientation Angle α_k
1	$\frac{2}{3}R$	0° (0)
2	$\frac{2}{3}R$	60° ($\pi/3$)
3	$\frac{2}{3}R$	120° ($2\pi/3$)
4	$\frac{2}{3}R$	180° (π)
5	$\frac{2}{3}R$	240° ($4\pi/3$)
6	$\frac{2}{3}R$	300° ($5\pi/3$)
7	0	-

that the subaperture tilt components scale is proportional to $(h/R) \times (r/R)$. This scaling with subaperture position is qualitatively correct since local wave-front slopes increase linearly with increased radial distance from the full aperture geometric center.

Similar (but tedious) algebraic procedures are employed to derive expressions for the full aperture modes $Z_4 - Z_{10}$.

These results are cast into the form of the sensitivity matrix S in Table II. The piston terms are not used and have been neglected. Examination of the sensitivity matrix S yields some rather interesting relationships between the full aperture Zernike modes and the corresponding subaperture modes:

(a) each full aperture mode A couples into only lower-order radial subaperture modes a_n (S is upper triangular);

(b) each full aperture mode A_n couples into the corresponding subaperture mode a_n with scaling coefficient $(r/R)^k$, where k is the highest power radial term in the nth mode;

(c) all full aperture modes couple into the subaperture tilt modes. Therefore, subaperture tilt information (only) from a sufficient number of subapertures is adequate to estimate the full aperture modes; (This is the basis of the Hartmann wave-front measurement technique.)

(d) without subaperture tilt data, subaperture focus and astigmatism as a minimum are required to estimate the full aperture modes except tilt.

The sensitivity results derived in this subsection are the basis for the full aperture calculations obtained in this section.

III. Full Aperture Zernike Mode Estimation

Wave-front aberrations in each subaperture are dependent on the aberration coefficients in the full aperture. It seems feasible, then, that, given enough subapertures, or given sufficiently detailed aberration information in a few subapertures, the full aperture aberrations could be estimated. We show in the sequel that this conjecture is true by illustrating two specific cases. In the first case, aberration measurements are taken from seven subapertures chosen to fill the full aperture as shown in Fig. 2. Aberration measurements $Z_1 - Z_{10}$ are assumed for each subaperture. We examine the accuracy of the full aperture aberration estimation error as a function of subaperture tilt uncertainty. These tilt uncertainties are mainly due to the difficulty of measuring and maintaining relative tilts of the subapertures. In the second case, aberration measurements are taken from a single on-axis subaperture.

A. Multiple Subapertures

Following the example used by Thunen and Kwon,[1] we use seven subapertures placed within the full aperture as shown in Fig. 2. Although the method is applicable for any number of Zernike mode measurements from each subaperture, here we assume that the Zernike coefficients for only the first ten modes are measured for each of these seven subapertures. Thus a total of seventy measurements is available for determining the unknown coefficients of the first ten full aperture Zernike modes. Mathematical equations for carrying out this procedure are now developed.

For the kth subaperture we have

$$\mathrm{S}_k\mathbf{A} = \mathrm{S}(\alpha_k, h_k)\mathbf{A} = \mathbf{a}^{(k)}, \tag{8}$$

where $\mathbf{A}$ is the 10-element vector of full aperture coefficients, $\mathbf{a}^{(k)}$ is the 10-element vector of coefficients for the kth subaperture, and S_k is a 10×10 sensitivity matrix. The values α_k and h_k, corresponding to the subaperture geometry shown in Fig. 2, are listed in Table III. An estimation error vector $\varepsilon_\mathbf{A}$ is defined as

$$\varepsilon_\mathbf{A} = \mathbf{b} - \mathrm{H}\mathbf{A}, \tag{9}$$

$$\mathbf{b} = \begin{bmatrix} \mathbf{a}^1 \\ \mathbf{a}^2 \\ \mathbf{a}^3 \\ \vdots \\ \mathbf{a}^7 \end{bmatrix} \quad \begin{bmatrix} \mathrm{S}_1 \\ \mathrm{S}_2 \\ \mathrm{S}_3 \\ \vdots \\ \mathrm{S}_7 \end{bmatrix}.$$

In this example, $\mathbf{b}$ is a 70-element vector, and H is a 70×10 element matrix. Our definition of the estimation error vector is consistent with standard treatments of weighted least-squares estimation (p. 121, Ref. 3). Following Maybeck,[3] we form the weighted least-squares scalar parameter J as

$$J = \varepsilon_\mathbf{A}^T \mathrm{W} \varepsilon_\mathbf{A} = (\mathbf{b} - \mathrm{H}\mathbf{A})^T \mathrm{W} (\mathbf{b} - \mathrm{H}\mathbf{A}). \tag{10}$$

The optimal estimate for $\mathbf{A}$ is defined as that estimate which minimizes J. The optimal estimate is determined by equating the partial derivative of J with respect to $\mathbf{A}$ equal to zero:

$$\frac{\partial J}{\partial \mathbf{A}} = \frac{\partial}{\partial \mathbf{A}} [(\mathbf{b} - \mathrm{H}\mathbf{A})^T W (\mathbf{b} - \mathrm{H}\mathbf{A})]$$

$$= -2(\mathbf{b} - \mathrm{H}\mathbf{A})^T \mathrm{W}\mathrm{H} = 0,$$

or

$$\mathrm{H}^T \mathrm{W}\mathrm{H}\mathbf{A} = \mathrm{H}^T \mathrm{W}\mathbf{b}.$$

Assuming that the matrix $\mathrm{H}^T\mathrm{W}\mathrm{H}$ is positive definite so that its inverse exists, we may uniquely solve for $\mathbf{A}$:

$$\mathbf{A} = (\mathrm{H}^T\mathrm{W}\mathrm{H})^{-1}\mathrm{H}^T\mathrm{W}\mathbf{b}$$

$$= Y\mathbf{b}, \tag{11}$$

where

$$Y = (\mathrm{H}^T\mathrm{W}\mathrm{H})^{-1}\mathrm{H}^T W. \tag{12}$$

It is well known in estimation theory (p. 121, Ref. 3) that, under the general assumption of zero-mean Gaussian additive measurement noise, a statistically optimum estimate for $\mathbf{A}$ is given by choosing the weighting matrix W to be the inverse subaperture wave-front measurement error covariance matrix:

$$\mathrm{W} = (\sigma_\mathrm{a}^2)^{-1}, \tag{13}$$

where

Table IV. Full Aperture Zernike Mode Inverse Covariance Matrix

$H^T W H =$

$\frac{7}{9}\frac{1}{\sigma_t^2}$	0	0	0	0	$\sqrt{2}\frac{32}{81}\frac{1}{\sigma_t^2}$	0	0	0	0
0	$\frac{7}{9}\frac{1}{\sigma_t^2}$	0	0	0	0	$\sqrt{2}\frac{32}{81}\frac{1}{\sigma_t^2}$	0	0	0
0	0	$\frac{32}{9}\frac{1}{\sigma_t^2}+\frac{7}{81}\frac{1}{\sigma^2}$	0	0	0	0	0	0	$\sqrt{15}(\frac{2}{3})^5\frac{1}{\sigma_t^2}$ $+\sqrt{15}\frac{40}{9^3}\frac{1}{\sigma^2}$
0	0	0	$\frac{144}{81}\frac{1}{\sigma_t^2}+\frac{7}{81}\frac{1}{\sigma^2}$	0	0	0	0	0	0
0	0	0	0	$\frac{144}{81}\frac{1}{\sigma_t^2}+\frac{7}{81}\frac{1}{\sigma^2}$	0	0	0	0	0
$\sqrt{2}\frac{32}{81}\frac{1}{\sigma_t^2}$	0	0	0	0	$\frac{3008}{3^6}\frac{1}{\sigma_t^2}+\frac{583}{9^3}\frac{1}{\sigma^2}$	0	0	0	0
0	$\sqrt{2}\frac{32}{81}\frac{1}{\sigma_t^2}$	0	0	0	0	$\frac{3008}{3^6}\frac{1}{\sigma_t^2}+\frac{583}{9^3}\frac{1}{\sigma^2}$	0	0	0
0	0	0	0	0	0	0	$(\frac{4}{3})^3\frac{1}{\sigma_t^2}+\frac{295}{9^3}\frac{1}{\sigma^2}$	0	0
0	0	0	0	0	0	0	0	$(\frac{4}{3})^3\frac{1}{\sigma_t^2}+\frac{295}{9^3}\frac{1}{\sigma^2}$	0
0	0	$\sqrt{15}(\frac{2}{3})^5\frac{1}{\sigma_t^2}$ $+\sqrt{15}\frac{40}{9^3}\frac{1}{\sigma^2}$	0	0	0	0	0	0	$\frac{5\cdot 2^5}{3^7}\frac{1}{\sigma_t^2}$ $+\frac{5\cdot 2^{12}}{3^8}\frac{1}{\sigma^2}$
1	2	3	4	5	6	7	8	9	10

Table V. Symbolic Representation for the Nonzero Elements of the Matrix H^TWH

A					G				
	A					G			
		B							H
			C						
				C					
G					D				
	G					D			
							E		
								E	
		H							F

Table VI. Symbolic Representation for the Full Aperture Zernike Coefficient Covariance Matrix $\sigma_A^2 = (H^TWH)^{-1}$

$\frac{D}{DA-G^2}$					$\frac{-G}{DA-G^2}$				
	$\frac{D}{DA-G^2}$					$\frac{-G}{DA-G^2}$			
		$\frac{F}{FB-H^2}$							$\frac{-H}{FB-H^2}$
			$\frac{1}{C}$						
				$\frac{1}{C}$					
$\frac{-G}{DA-G^2}$					$\frac{A}{DA-G^2}$				
	$\frac{-G}{DA-G^2}$					$\frac{A}{DA-G^2}$			
							$\frac{1}{E}$		
								$\frac{1}{E}$	
		$\frac{-H}{FG-H^2}$							$\frac{B}{FB-H^2}$

$$\sigma_a^2 = \begin{bmatrix} \sigma_a^2(1) & 0 & 0 \\ 0 & \sigma_a^2(2) & 0 \\ 0 & 0 \ddots & 0 \\ & & \sigma_a^2(7) \end{bmatrix}$$

Note: superscripts denote subaperture number.

If each measurement error is statistically independent, σ_a^2 is a diagonal matrix, and $W_i = 1/\sigma_i^2$. The estimation error associated with the optimal estimate is given by

$$\begin{aligned} \sigma_A^2 &= Y\sigma_a^2 Y^T \\ &= (H^TWH)^{-1}H^TW\sigma_a^2W^TH(H^TWH)^{-1} \\ &= (H^TWH)^{-1} \end{aligned} \tag{14}$$

by use of Eq. (13) and the fact that $W = W^T$. Equation (14) indicates how the full aperture Zernike mode coefficient estimation errors can be calculated with the knowledge of the subaperture coefficient estimation errors and the sensitivity matrices $S(\alpha_k,h_k)$. This calculation is performed for the case that the ith subaperture error matrix $\sigma_a^2(i)$ is of the form

$$\sigma_a^2(i) = \begin{bmatrix} \sigma_t^2 & & & 0 \\ & \sigma_t^2 & & \\ & & \sigma^2 & \\ & & & \ddots \\ 0 & & & \sigma^2 \end{bmatrix}, \tag{15}$$

where σ_t^2 represents the measurement error variance of the tilt component, and σ^2 represents the measurement error variance of the nontilt Zernike terms. The measurement errors of the various Zernike coefficients are assumed to be uncorrelated.

The 10×10 matrix σ_A^2 has been explicitly calculated by algebraic methods. This approach allows us to analytically determine which factors influence the estimation and provides a comparison case for the simulation results calculated by Thunen and Kwon.[1] The block diagonal form of the W matrix and partitioned matrix form of the H matrix allow expression of the matrix H^TWH in the alternative form more amenable for calculation:

$$H^TWH = \sum_{k=1}^{7} S^T(\alpha_k,h_k)\sigma_a^2 S(\alpha_k,h_k). \tag{16}$$

The azimuthal symmetry of the $S(\alpha_k,h_k)$ terms, when averaged in Eq. (16), yield the sparse matrix in Table IV. The H^TWH matrix is the inverse covariance matrix for the ten full aperture Zernike mode coefficients. The matrix is sufficiently sparse that its matrix inverse can be reasonably calculated in terms of its nonzero elements. A single symbolic representation for each nonzero matrix element as shown in Table V has been defined to facilitate the calculation. The inverse matrix $(H^TWH)^{-1}$ is given in Table VI. The diagonal elements represent the covariances of the individual full aperture Zernike coefficients estimated on the basis of ten Zernike mode measurements for each of the seven subapertures. For example, the covariance of the first-order astigmatism term A_4 is (from Tables IV–VI)

$$\begin{aligned} \mathrm{cov}(A_4) = \frac{1}{C} &= \left(\frac{144}{81}\frac{1}{\sigma_t^2} + \frac{7}{81}\frac{1}{\sigma^2}\right)^{-1} \\ &= \frac{81\sigma_t^2\sigma^2}{144\sigma^2 + 7\sigma_t^2}. \end{aligned} \tag{17}$$

Equation (17) shows the variation in full aperture astigmatism with subaperture tilt (σ_t^2) and higher-order aberrations (σ^2). As σ_t^2 becomes large, the $\mathrm{cov}(A_4)$ reaches an asymptotic value of $81\sigma^2/7$, while as σ_t^2 is made smaller, $\mathrm{cov}(A_4)$ asymptotically approaches $81\sigma_t^2/144$. Thus improved subaperture tilt measurements do provide improved full aperture astigmatism estimates. The converse is not true, however, since the full aperture astigmatism error cannot be larger than $81\sigma^2/7$ no matter how large the subaperture tilts may be. Similar results have been derived for the other full aperture Zernike modes. Full aperture Zernike mode estimation errors for various subaperture tilt accuracies are given in Table VII for the case that ten Zernike modes are measured to an accuracy of 0.006λ for each of the seven subapertures.

The focus (A_3) and fourth-order spherical aberration (A_{10}) values tabulated are the rms errors associated with these coefficients, while astigmatism (A_4 and A_5), coma (A_6 and A_7), and clover (A_8 and A_9) values are each the rms of two coefficients rms error comprising the two orthogonal axes of these modes. The total rss (root sum square) wave-front measurement, focus, and astigmatism errors are plotted in Fig. 3.

Table VII. Full Aperture Zernike Mode Estimation Accuracy as a Function of Subaperture Tilt Measurement Error (Ten-Full Aperture Modes Estimated Using Seven Subapertures with Ten Modes Each, $\sigma_{a_i} = 0.006\lambda$ $i > 3$)

	FULL APERTURE (Standard Deviation Waves)						
Subaperture Tilt	Total RSS	Focus	Astigmatism	Coma	Clover	Spherical	Tilt (single axis)
0.0001λ	0.0034λ						
0.0003	0.0035	0.0005	0.0003	0.0002	0.0003	0.0034	0.00036
0.001	0.0038						
0.003	0.006	0.0017	0.0031	0.0021	0.0026	0.0034	0.0036
0.01	0.015						
0.03	0.029	0.012	0.020	0.0087	0.012	0.0034	0.034
0.1	0.037						
0.3	0.039						
1.0	0.039	0.02	0.028	0.0094	0.013	0.0034	1.13

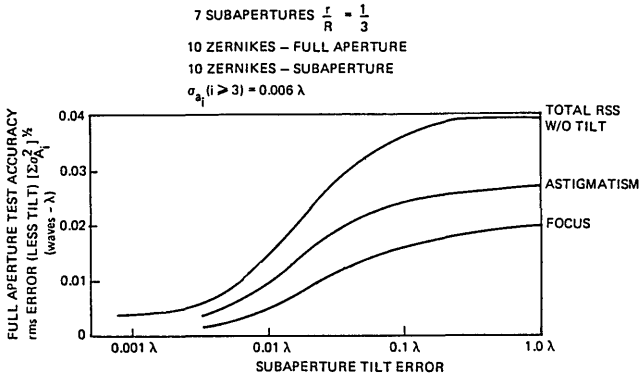

Fig. 3. Effect of subaperture tilt measurement error on full aperture test accuracy.

Table VIII. Full Aperture Zernike Mode Estimation Accuracy as a Function of Subaperture Tilt Measurement Error (Ten-Full Aperture Modes Estimated Using Seven Subapertures with Five Modes Each, $\sigma_{a_i} = 0.006\lambda$ $i > 3$)

	FULL APERTURE (Standard Deviation Waves)						
Subaperture Tilt	Total RSS	Focus	Astigmatism	Coma	Clover	Spherical	Tilt (single axis)
0.0001λ	0.0037λ						
0.0003	0.0038	0.0006	0.0003	0.0002	0.0021	0.0037	0.00035
0.001	0.0041						
0.003	0.0062	0.0017	0.0032	0.0021	0.0027	0.0037	0.0036
0.01	0.0152						
0.03	0.0292	0.0125	0.021	0.0087	0.012	0.0037	0.034
0.1	0.0377						
0.3	0.0390						
1.0	0.0392	0.02	0.028	0.0095	0.0135	0.0037	1.13

Table IX. Full Aperture Zernike Mode Estimation Accuracy as a Function of Subaperture Tilt Measurement Error (Ten-Full Aperture Modes Estimated Using Seven Subapertures with Ten Modes Each, $\sigma_{a_i} = 0.006\lambda/\sqrt{10}$ $i > 3$)

	FULL APERTURE (Standard Deviation Waves)						
Subaperture Tilt	Total RSS	Focus	Astigmatism	Coma	Clover	Spherical	Tilt (single axis)
0.0001λ	0.0011						
0.0003	0.0012	0.0002	0.0003	0.0002	0.0003	0.0011	0.00036
0.001	0.0019						
0.003	0.0045	0.0016	0.003	0.0018	0.0023	0.0011	0.0035
0.01	0.0094						
0.03	0.0118	0.0060	0.0088	0.0030	0.0042	0.0011	0.034
0.1	0.0123						
0.3	0.0124						
1.0	0.0124	0.0065	0.0091	0.0030	0.0042	0.0011	1.13

B. Estimation Properties

Several quantitative properties of the estimation process are examined. First we address the consequences of using fewer aberration measurements in each subaperture. Then we calculate estimation error accuracy bounds and their variation with measurement accuracy.

As many more measurements are available than quantities being estimated, accurate full aperture estimation might also be possible with fewer aberration measurements from each subaperture. We tested this conjecture by using only five aberration measurements from each subaperture.

The test case was repeated using only five Zernike modes in each subaperture. These test results are given in Table VIII and are nearly identical to the ten mode case.

The minor differences that did occur between the ten and five subaperture mode cases were a shift in the spherical aberration estimation accuracy and a degradation in focus estimation accuracy at small tilts. Otherwise, no discernible difference occurred for large subaperture tilt errors.

This result suggests a simple calculation can be used to establish the fundamental accuracy lower bounds for aberration modes. Because the sensitivity matrices are upper triangular, no improvement in full aperture coefficient estimation accuracy is obtained by including subaperture modes higher than the full aperture mode to be estimated. For example, a bound on focus estimation accuracy is given by a 3×3 (tilt, tilt, focus) estimation problem. Again, because the sensitivity matrices are upper triangular, the matrix $[\sigma_A^2(3 \times 3)]^{-1}$ has already been computed and is given simply as the upper-left 3×3 submatrix of $H^T W H$ in Table IV. It is repeated below for convenience and clarity:

$$[\sigma_A^2(3 \times 3)]^{-1} = H^T W H_{3\times 3} = \begin{bmatrix} \frac{7}{9}\frac{1}{\sigma_t^2} & 0 & 0 \\ 0 & \frac{7}{9}\frac{1}{\sigma_t^2} & 0 \\ 0 & 0 & \frac{32}{9}\frac{1}{\sigma_t^2} + \frac{7}{81}\frac{1}{\sigma^2} \end{bmatrix}. \quad (18)$$

The matrix inverse of this diagonal matrix is readily calculated by inspection. The focus error variance is

$$\mathrm{cov}(A_3) = \left[\frac{32}{9}\frac{1}{\sigma_t^2} + \frac{7}{81}\frac{1}{\sigma^2}\right]^{-1} = \frac{81\sigma_t^2\sigma^2}{32(9)\sigma^2 + 7\sigma_t^2}. \quad (19)$$

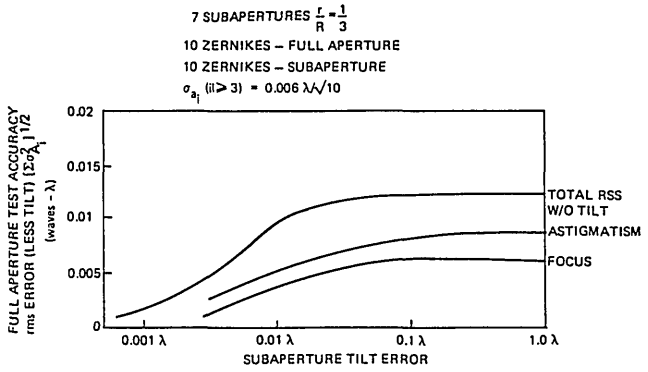

Fig. 4. Effect of subaperture tilt measurement error on full aperture test accuracy.

It follows from Eq. (19) that the rms focus error for large subaperture tilts is given by

$$[\cos(A_3)]^{1/2}_{\sigma_t^2\to\infty} = \sqrt{\frac{81}{7}}\,\sigma = 3.4\sigma = 0.02\lambda \text{ at } (\sigma = 0.006\lambda). \quad (20)$$

The value agrees with the focus estimation error values presented Tables VII and VIII for the case that ten full aperture modes are estimated.

The focus aberration estimate bound can also be compared for finite subaperture tilt uncertainty. At $\sigma_t = 0.0003\lambda$ and $\sigma = 0.006\lambda$ the focus estimation error is

$$[\mathrm{cov}(A_3)]^{1/2}_{\sigma_t=0.006\lambda} = \left[\frac{32}{9}\frac{1}{(0.0003\lambda)^2} + \frac{7}{81}\frac{1}{(0.006\lambda)^2}\right]^{-1/2} = 0.00016\lambda,$$

which compares with the value 0.0005λ obtained in the mode estimation case. The focus error calculated for this 3×3 case is an estimation error lower bound. As additional full and subaperture modes are considered, cross correlations between focus and the higher-order modes—in particular, spherical aberration—degrade the focus error estimation accuracy.

The full aperture test accuracy results shown in Fig. 3 characterize accuracy variations with subaperture tilt measurement error. We should also characterize test accuracy variation with changes in the other aberration measurements. The focus accuracy bound results in Eqs. (19) and (20) suggest that, at large subaperture tilts, the full aperture accuracies vary linearly with nontilt subaperture measurement error. The full aperture aberration estimation problems were repeated with σ_i reduced by $\sqrt{10}$. The results are given in Table IX and plotted in Fig. 4. We see by comparison of Tables VII and IX that our conjecture is correct—the full aperture aberration coefficient estimates are reduced by the factor of $\sim\sqrt{10}$.

C. Error Model Insights

Several useful insights have been gained through examination of the numerical results obtained via algebraic formulation of the multiple-subaperture optical test concept. These insights relate to the physical process by which full aperture coefficients are estimated from the subaperture measurements.

The optimal estimation formulation in Sec. III develops a linear transformation Y between the subaperture measurement vector $\mathbf{a}$ and the unknown full aperture coefficient vector $\mathbf{A}$. The linear transformation Y given by Eq. (12) depends only on the composite sensitivity matrix H and the measurement error covariance matrix W. The transformation Y exists provided that the matrix inverse $(\mathrm{H}^T\mathrm{WH})^{-1}$ exists, which is assured if H has full rank. Physically this means that each full aperture mode induces a measured subaperture coefficient response which is linearly independent of the responses induced by all other full aperture Zernike aberrations considered. The composite sensitivity matrix H has as it subpartitions the sensitivity matrices $\mathrm{S}(\alpha_k, h_k)$. Therefore, desirable properties of H depend directly on the size, placement, and number of subapertures.

A major trade-off exists between the number of subapertures used and the number of Zernike aberration modes measured in each subaperture. The advantage of a large number of apertures is that averaging their independent measurement errors tends to reduce the full aperture estimation error by the square root of the number of measurements N. A disadvantage of a large number of subapertures is that aperture size (and the ratio r/R) goes down in proportion to $1/\sqrt{N}$. The reduction in subaperture size reduces sensitivity to full aperture modes and leads to amplification of subaperture measurement noise in the estimation process.

The net result is a loss in accuracy for the full aperture measurements as illustrated by the 3×3 example in Sec. II.B. From Eq. (18), the full aperture single-axis tilt variance is given by $9/7\ \sigma_t^2$ and in general by $(R/r)^2/N\sigma_t^2$, where R/r is the ratio of full-to-subaperture radii, and N is the number of subapertures. For nonoverlapping subapertures, geometrical constraints require that $(R/r)^2 \geq N$, and consequently the full aperture tilt coefficient measurement error is always greater than the single subaperture tilt coefficient uncertainty.

Trade-offs relating to the number of subaperture Zernike modes used are most sensitive to which low-order modes are used rather than the total number of modes. Noise sensitivity favors use of the low-order modes tilt, focus, and astigmatism rather than the higher-order radial modes. This sensitivity is best illustrated by consideration of a single centered subaperture.

D. Single Subaperture

In theory, full aperture aberration error estimates can also be made from a single subaperture arbitrarily placed in the full aperture. Single subaperture results can be derived from the sensitivity matrix presented in Table II. The results are algebraically unwieldy, however, except for the special case of a single central subaperture. It is instructive to carry out this case to

Table X. $(H^T W H)^{-1}$ for Single Central Subaperture

	1	2	3	4	5	6	7	8	9	10
1	$(\frac{R}{r})^2\sigma_t^2+8(\frac{R}{r})^2[(\frac{R}{r})^2-1]^2\sigma^2$					$2\sqrt{2}(\frac{R}{r})^4[(\frac{R}{r})^2-1]\sigma^2$				
2		$(\frac{R}{r})^2\sigma_t^2+8(\frac{R}{r})^2[(\frac{R}{r})^2-1]^2\sigma^2$					$2\sqrt{2}(\frac{R}{r})^4[(\frac{R}{r})^2-1]\sigma^2$			
3			$(\frac{R}{r})^4\sigma^2$							
4				$(\frac{R}{r})^4\sigma^2$						
5					$(\frac{R}{r})^4\sigma^2$					
6						$(\frac{R}{r})^6\sigma^2$				
7							$(\frac{R}{r})^6\sigma^2$			
8								$(\frac{R}{r})^6\sigma^2$		
9									$(\frac{R}{r})^6\sigma^2$	
10										$(\frac{R}{r})^8\sigma^2$

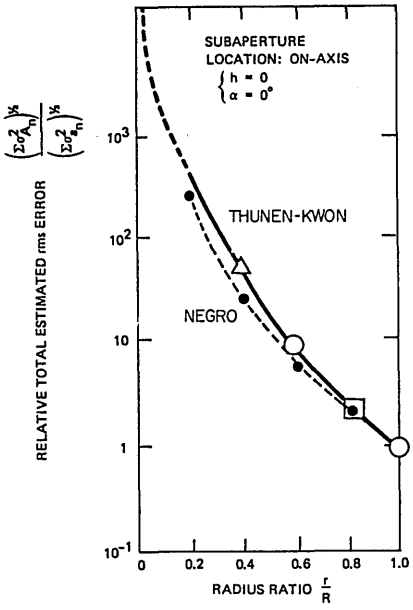

Fig. 5. Full aperture wave-front estimation accuracy degradation as a function of subaperture radius for a single central subaperture.

determine how estimation accuracy degrades with reduced subaperture size and to provide a direct numerical comparison with the Thunen-Kwon results. The methodology developed in Sec. III.A is adopted for this analysis.

The sensitivity matrix was determined for $h = 0$ and used to calculate the full aperture covariance matrix in Table X. The table explicitly shows noise amplification by the factor $(R/r)^{2k}$, where k is the radial order of the mode. The ratio of rms full aperture wave-front error to subaperture wave-front error excluding tilt is, using Table X,

$$\left[\frac{\Sigma\,\sigma_{Ai}^2}{\Sigma\,\sigma_{ai}^2}\right]^{1/2} = \frac{1}{10}\left\{2\left(\frac{R}{r}\right)^2 + 16\left(\frac{R}{r}\right)^2\left[\left(\frac{R}{r}\right)^2 - 1\right]^2 + 3\left(\frac{R}{r}\right)^4 + 4\left(\frac{R}{r}\right)^6 + \left(\frac{R}{r}\right)^8\right\}.$$

This ratio is plotted in Fig. 5 as a function of r/R and illustrates the amplification of subaperture measurement noise, especially at large values of R/r.

Also plotted in Fig. 5 are similar results derived numerically by Thunen and Kwon for the case of 15 Zernike modes. Good agreement between the results is obtained, except at low ratios of r/R, where contributions of modes 11–15, not included in my analytic result, dominate.

One interesting feature of the full aperture Zernike mode estimation data in Tables VII–IX is that the spherical aberration accuracy is independent of subaperture tilt. Apparently, the seven subaperture tilt measurements are not sufficient to distinguish spherical aberration and focus due to undersampling. These estimates are correlated as indicated by the nonzero off-diagonal element $(H^TWH)^{-1}{}_{3,10}$ in Table VI. The first-order independence of the spherical aberration estimation error with subaperture tilt also explains why full aperture rms accuracy approaches a nonzero asymptote as subaperture tilt is reduced. In the ten coefficient examples considered here, the spherical aberration residual estimation error is the dominant contributor to overall full aperture wave-front rms error for small subaperture tilt uncertainties. Its contribution can be reduced only by improvement of subaperture coefficient measurement accuracy or by use of more than seven subapertures to enhance the observability of the spherical aberration.

IV. Conclusions

An innovative approach for testing large optical apertures with multiple subapertures has been examined in detail. Algebraic sensitivity models characterizing the relationship between full aperture aberration modes and subaperture modes have been explicitly calculated for a ten Zernike mode case. These models were used to numerically illustrate the full aperture estimation process.

A number of issues require further investigation. Treatment of discontinuous wave fronts, alternative wave-front representation polynomials, and characterization of measurement errors in terms of detection SNRs, is strongly encouraged. We also recommend (1) the investigation of test self-check techniques by calculation of error residuals, (2) the investigation of unmodeled and higher-order aberration effects, and (3) the analysis of static subaperture tilt estimation techniques and the utility these data might provide.

References

1. J. G. Thunen, O. Y. Kwon, "Full Aperture Testing With Subaperture," Proc. Soc. Photo-Opt. Instrum. Eng. **351**, 19 (1983).
2. O. Y. Kwon, J. G. Thunen, "LODE: Subaperture Optical Testing," LMSC D811929, 6 Nov. 1981.
3. P. S. Maybeck, *Stochastic Models, Estimation and Control, Vol. 1* (Academic, New York, 1979).

The author wishes to acknowledge the technical contributions and enlightening discussions with John Thunen and Osuk Kwon whose creative work led to the research reported here. Special recognition is also due to graduate student Rich Mozzicato, who performed many of the tedious algebraic manipulations, and to Lisa Gorman, who professionally prepared the manuscript.

This work was performed under the sponsorship of the Defense Advanced Research Projects Agency.